Structural, optical and electrical properties evaluation of PPY-CuO nanocomposite for OLEDs as electron transport layer material.

[1]U. Das, [2]Rohit Kandulna*,[1]Rimpi,[3]B. Kachhap,[1]Janardan Choudhary

[1]Department of Physics YBN University, Ranchi

[2]Department of Physics, IIIT Ranchi

[3]University Department of Botany, Ranchi University, Ranchi.

*Corresponding author e-mail: rohitkandulna4@gmail.com

Abstracts

The PPY-CuOnanocomposites was synthesized by chemically oxidatively polymerizing pyrrole monomer. The FESEM, TEM and XRD examination revealed the structural properties of the CuO, PPY and PPY-CuOnanocomposites. Increased radiative charge carrier recombination was observed in the PPY-CuO nanocomposite. As resistivity dropped, the recombination in radiative form increased for the PPY-CuO nanocomposite. When compared to the original CuO, the PPY-CuO nanocomposite was shown to have an improved current density of 11.36 A/cm^2 .It was discovered that the PPY-CuO nanocomposite had higher rates of radiative recombination, improved conductivity&electron mobility, and higher luminescence in the visible spectrum, indicating that it could be used as an electron transport layer (ETL) material in organic light emitting diodes (OLEDs).

Keywords: PPY-CuOnanocomposite, optical-electrical properties, OLEDs, ETL.

Introduction

For usage in optoelectronic device applications, organic-inorganic nanocomposites based on intrinsically conductive polymers demonstrate exceptional advances. The OLEDs have been

acknowledged as practical alternatives for uses using green energy [1]. OLEDs have drawn a lot of interest from scientists and the display technology business [2, 3]. Due to its numerous beneficial qualities, such as their planar nature, brilliant colours, luminescent display with vast area, broad viewing angle, minimal driving voltage, low production cost, and high resolution, polymeric hybrid nanocomposite-based OLEDs are the most popular light-emitting instrument [4, 6]. Additionally, the stability and efficiency of OLED performance have long been constrained. Power efficiency is one of the most important factors in display technology, and blue light producing devices perform poorly in comparison to red and green light [7]. OLED device structure's strong applied potential reduces power efficiency. To overcome the aforementioned drawbacks, OLEDs are constructed as layered structures containing an emission layer, a hole transporting layer, and an electron transporting layer [8]. The cathode (negative side) and anode (positive side) of a battery or an electrical current supply the driving voltage. In the emissive layer, the recombined electrons and holes produce excitons, which are then transformed to light [9]. By using a hopping mechanism, the electron transporting layer (ETL) makes it easier for electrons to flow from the electrode (cathode) to the electroluminescent emissive layer (EML). The electron-injection layer and the electron-transfer layer are interlayers that sublimated one another through chemical processes [10]. ETL is the preeminent framework for enhancing the performance of OLEDs with strong features. The following qualities must exist in the material for ETL: (1) Accelerated charge carrier recombination, (2) High reversible electrochemical reduction potential, (3) Low band gap value and High conductivity high electron transport mobility and thermal stability, and (5) brightness below the visible spectrum. With organic-inorganic nanocomposites, attention must be paid to the aforementioned characteristics. Research into alternative energy sources has increased dramatically in response to the growing need for renewable energy [11–15]. Organic-inorganic hybrid nanocomposites are new cutting-edge

materials that blend different inorganic and organic component properties. Particularly polymer-based hybrid nanocomposites provide a radical alternative to traditional polymer nanocomposites by reinforcing polymers with a second inorganic phase consisting of carbon material [16]. Different conductive polymers, including polypyrrole (PPY), polypyrenes (PPR), polyindole (PIN), polyethylene (PTP), poly phenylene vinylene (PPV), polyaniline (PANI), and others, have evolved the outcomes of inorganic therapy [17]. Since they are simple to polymerize and have strong thermal and environmental durability, polypyrrole and its derivatives have garnered a lot of attention as a potential material for opto-electronic devices. The cation radicals that make up PPY's chemical structure boost both electrical and environmental friendliness [18]. However, bare PPY exhibits a poor capacity for adsorption and has a propensity to cluster through interaction with -, which leads to insufficient utilization of bare PPY. It is anticipated that creating hybrid nanocomposites based on PPY will be an effective way to combat aggregation and increase their adsorption ability in order to address this issue. It is discovered that the hybrid nanocomposites of metal oxide/sulphides (CdS, ZnO, MnO_2, CuO) with PPY show intelligent performance. In particular, CuO (Copper oxide) has the strong qualities that make it a good choice for use in optoelectronic and supercapacitor systems. While PPY is a p-type material and CuO is a monoclinic n-type material, their hybrid nanocomposites can create band gaps, conductivities, and specific capacitance values that are all tunable [19]. CuO has good mechanical flexibility and environmental stability, and its acid/base (doping/un-doping) characteristics can be used to modify its resistivity [20]. CuO also exhibits a 60 MeV binding energy excitation and a small band gap energy of 1.5 to 1.8 eV [21]. The enhanced features measurement of the PPY-CuO-rGO nanocomposite for usage as an ETL material in OLEDs is highlighted in the current study.

2. Experimental

2.1 Synthesis of polypyrrole (PPY)

Using the COP technique, the pyrrole monomer was polymerized to create the PPY. To maintain a stoichiometric ratio of 1:2, 0.2 M of pyrrole monomer was first added to 0.4 M of APS in 110 mL DI water. The entire setup was maintained at a constant temperature of 0 to 5 °C for 11 hours while being continually agitated. The collected, completely black precipitate was placed in a refrigerator for 21 hours to complete the polymerization process. The resultant precipitate was subsequently 4-5 times washed with ethanol and DI water. Additionally, it was dried for 25 hours at 60 °C in the oven.

2.2 Synthesis of copper oxide (CuO) nanoparticle

$CuCl_2$ and $Cu(NO_3)_2.3H_2O$ were combined to create CuO nanoparticles using precipitation techniques. Precursor was first added to 90 mL of DI water to create a 0.1 M concentration. NaOH solution (0.1 M) was gently dissolved while being vigorously stirred until pH tended to 14. Three to four times each with DI water and ethanol, the collected black precipitates were cleaned until the pH was 7. Following filtration, the precipitates underwent 20 hours of 60 °C drying and 4 hours of 450 °C calcination.

2.3 Synthesis of PPY-CuOnanocomposite

65 mL of DI water and 0.2 M pyrrole monomer were first combined. The aforementioned solution was eventually supplemented with the 15% CuO. A 30 mL solution containing 3.5 g of APS was also created and added dropwise to the pyrrole solution. The complete system was kept spinning continuously for six hours in the ice bath chamber. Three to four cycles of

ethanol and DI water filtration were performed on the acquired dark black precipitate. The filtered precipitate was then stored in a vacuum oven for 30 hours at 70 °C.

2.4 Measurement techniques

The structural properties of GO, PPY, CuO, PPY-CuO, and PPY-CuO-rGO nanocomposites were examined using an X-ray diffractometer (XRD) in the 2 angular range of 10° to 80°. (GBCMMA as model). The surface structure was examined using energy dispersive X-ray (EDX) and field emission scanning electron microscopy (FESEM) (models: ZEISS, SUPRA-55, and SDD X MAX 50 EDS, respectively). A thorough morphological investigation was carried out utilising transmission electron microscopy (TEM) at 200 KeV (model: CM 200). The UV-Vis spectroscopic method (model: CARY-5000) was used to measure ultraviolet-visible absorption in the 200 nm to 800 nm wavelength range. A fluorescence spectrophotometer (model: Hitachi F-2500 Fluorescence Spectrophotometer) was used to assess the photoluminescence (PL) spectroscopy and time-resolved PL spectra, with an emission range of 350 nm–500 nm and an excitation energy of 320 nm. The current density-voltage (J-V) relationship was measured by the source meter (KEITHLEY 2400 model).

3. Result and discussion

3.1 FESEM analysis

Fig.1(a-c) displays the FESEM images for the CuO, PPY and PPY-CuO nanocomposites. The FESEMimage ofCuO nanoparticle revealed random surface grain dispersion with a mostly trapezium grain structure. The PPY showed a spherical ball form and was evenly distributed across the surface [22]. The aggregation in the PPY polymer chain was accelerated by the anisotropic fashionof CuOas indicated in Fig.1c.

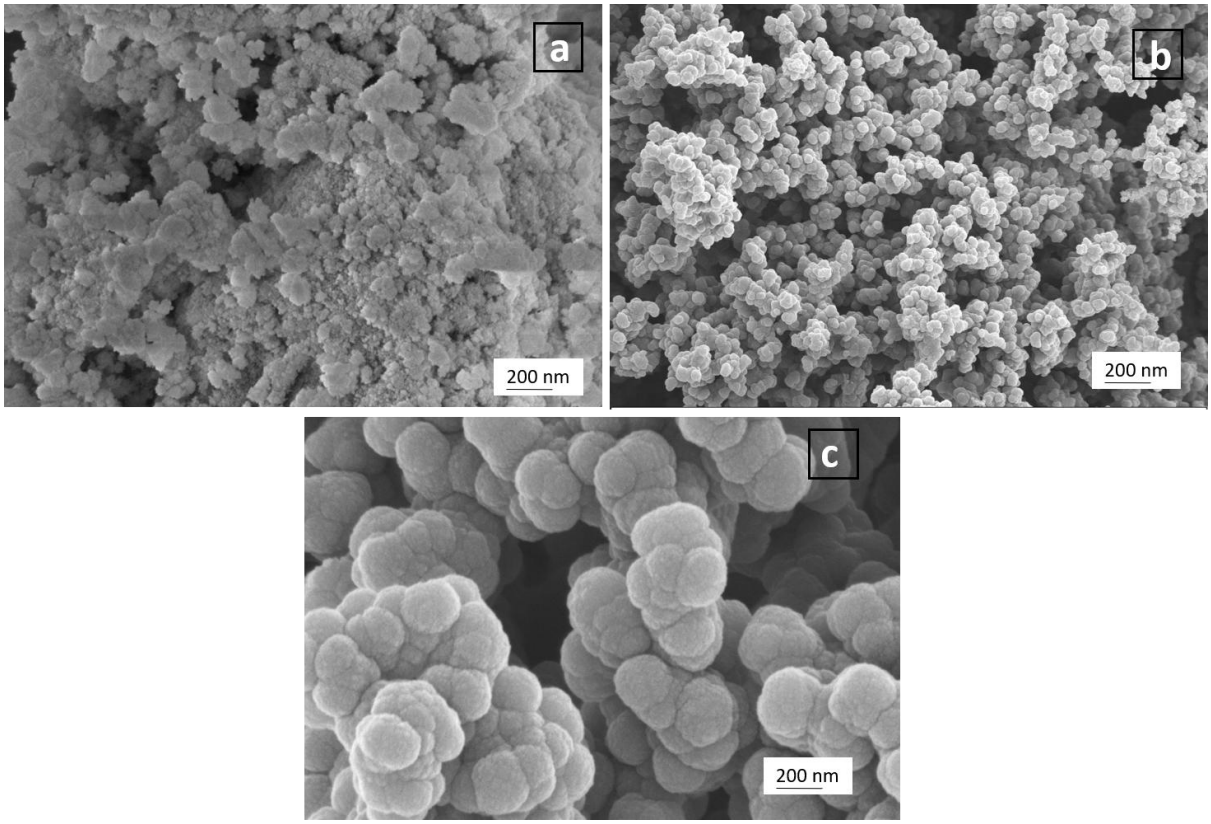

Fig. 1: The FESEM images of (a) CuO, (b) PPY, and (c)PPY-CuOnanocomposite.

3.2 TEM analysis

Fig.2 displays TEM images of the CuO and PPY-CuO nanocomposites. The TEM picture of CuO showed a mostly trapezoidal grain shape with random surface grain dispersion and observed to be good agreement to the FESEM images. In PPY-CuO hybrid nanocomposite, it was found that the insufficiently dense PPY was encased over the denser CuO nanofillers. The interlinking of PPY's amines group with Cu ions resulted in the non-homogenous random trapezium grain structure in the PPY-CuO nanocomposites that were seen in TEM images being enclosed by a PPY coated layer. The average particle size was observed ~ 46 nm for the PPY-CuO nanocomposite

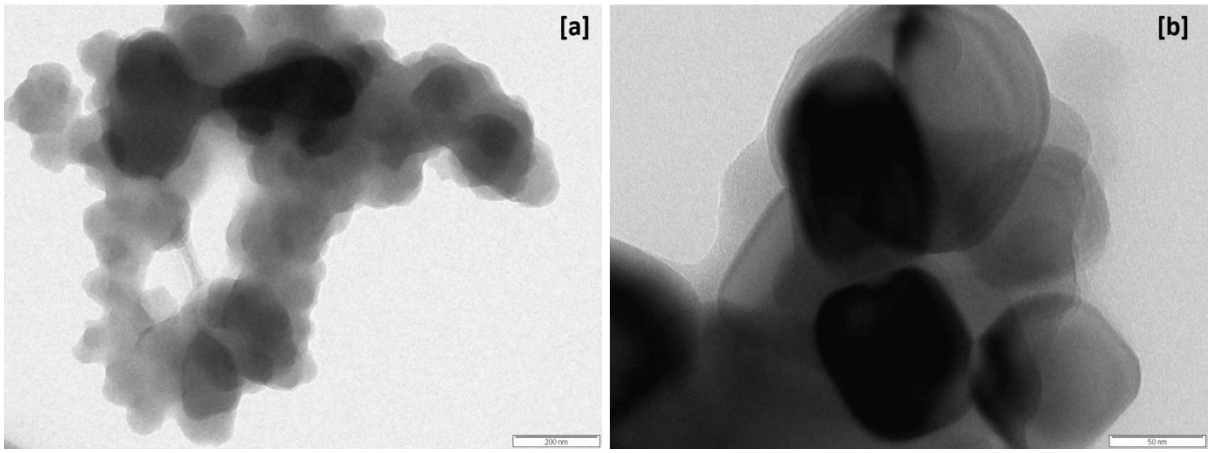

Fig. 2: TEM images for (a) CuO,and (b) PPY-CuO nanocomposite.

3.3XRD Analysis

Fig.3 displays the XRD spectrum for the PPY, CuO and PPY-CuOnanocomposite. The PPY XRD pattern demonstrated that it was amorphous because of a partial synergetic interaction between the PPY polymer matrix and the big diffraction peak at 24.15° [23]. Meanwhile, the monoclinic system of single phase CuO was clearly seen in the diffraction bands of CuO nanofillers [24]. The CuO crystallinity was best measured in its strong peaks. The observed lattice's parameters were a = 4.84, b = 3.47, and c = 5.33, and the band's strength and position were in good agreement with JCPDS data (card no. 05-0661). The PPY-CuO diffraction pattern showed tiny PPY humps at 23.6° and a crystalline band of CuO nanofillers and spectrum supported the successful synthesis of PPY-CuO nanocomposites.

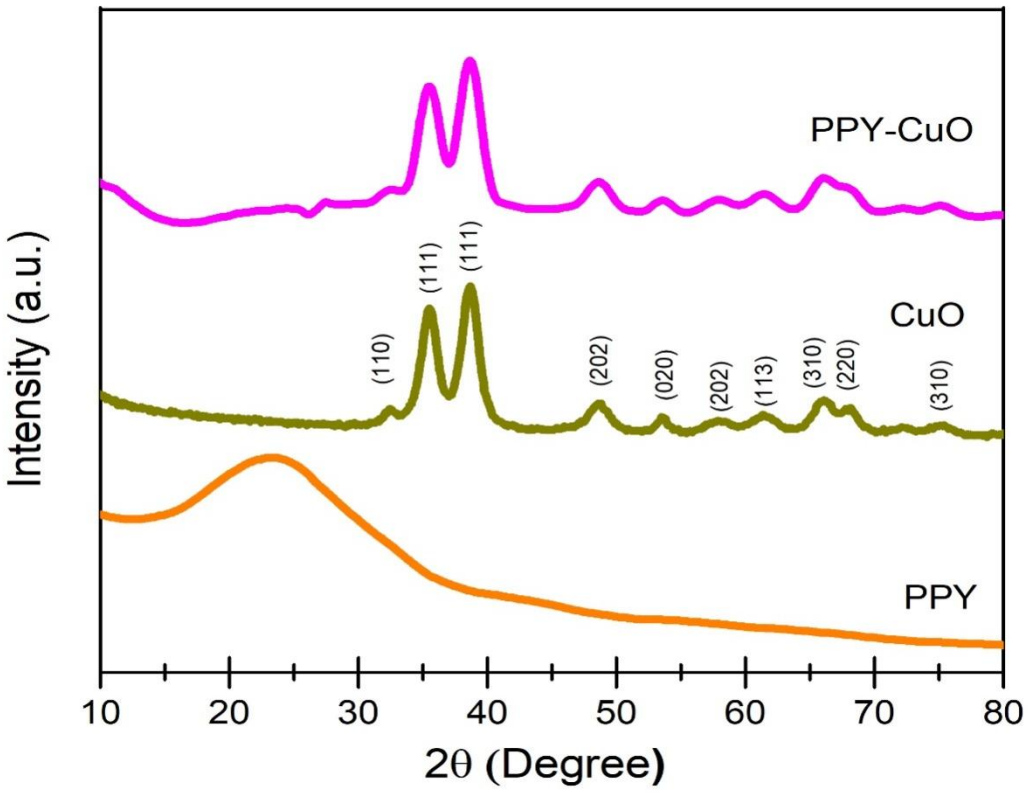

Fig. 3: X-ray diffraction patterns ofPPY, CuO, and PPY-CuOnanocomposite.

3.4PLanalysis

The CuO and PPY-CuOnanocomposites' PL emission spectra at 330 nm excitation energy are shown in Fig. 4. The xenon-arc lamp provided the excitation energy. The PL spectra showed three visible emission peaks with UV centre bands at 434 nm (violet), 466 nm (blue), and 534 nm (green). The UV area band emission is assumed to be caused by the non-radiative annihilation of excitons, whereas the visible emission is thought to be caused by the radiative recombination of an electron filling the oxygen vacancy with a photogenerated hole [25]. Due to the well-defined bandgap of the CuO material and the recombination of excitons at this peak, a narrow UV emission band was visible [26]. While the deep level flaws of the CuO nanofillers were associated with three distinct emission peaks in the visible spectrum. The transitions from CuO deficits to the O_2 2p band were attributed to the violet band at 434 nm

[27]. The blue emission band in PPY-CuO nanocomposites and the recombination of deep-defect electrons and extra holes may originate from ionized oxygen vacancies in the VB. The green emission band is caused by the recombination of electrons and holes, and it is trapped in oxygen-related defects in the conduction band [28]. By eliminating oxygen vacancies and surface defects at the heterojunction between PPY and CuO the interbond radiative recombination may be stopped. The relativelyhigh radiative electron-hole recombination was responsible for the optimal PL intensity for PPY-CuO nanocomposites.

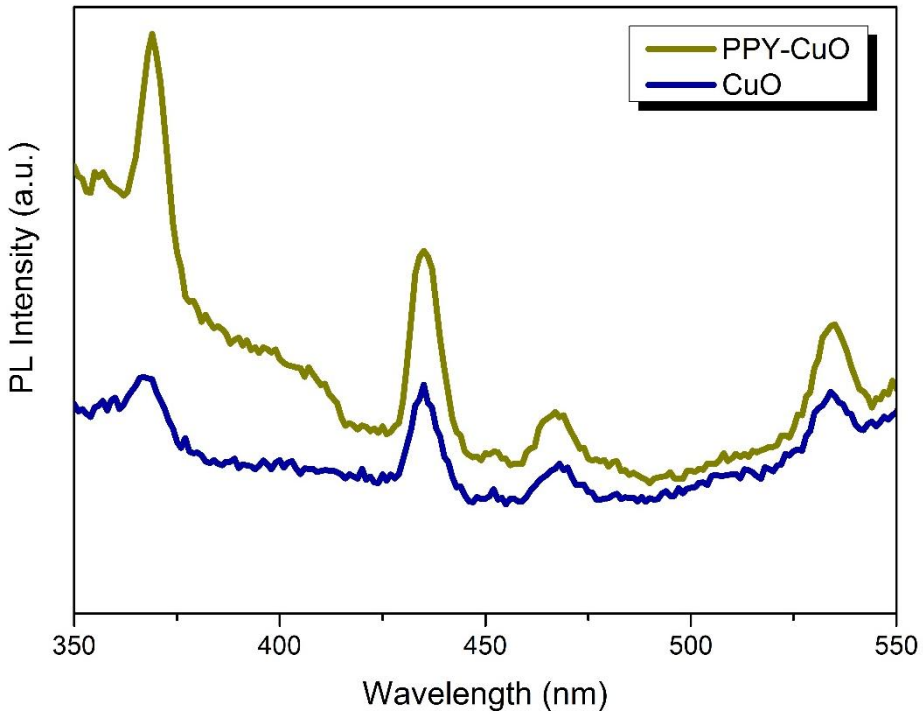

Fig. 4: Photoluminescencespectrafor CuO and PPY-CuOnanocomposite

3.5 Current density-voltage (J-V) measurement

Fig.5 showed the J-V curves for CuO and PPY-CuO nanocomposite. The data was gathered in the potential range of -8 V to +8 V at room temperature. The ohmic behavior was visible in all measurements. In the first step, spin coating was used to coat the CuO and PPY-CuOnanocomposite in ITO glass as it had been made. While the pristineCuO showed the

relatively lowest current density at 5.39 A/cm^2, the incorporation of CuO into PPY boosted the current density. Theoptimized higher current density of 11.36 A/cm^2 was observed PPY-CuO nanocomposite. The increase in current density was brought on by the high degree of electron mobility. The longevity of minority charge carriers has an impact on the rate of charge carrier recombination as well as increasing radiative electron-hole recombination. As a result, the PPY-CuO nanocomposite's resistivity reduced and the rate of radiative recombination was accelerated.

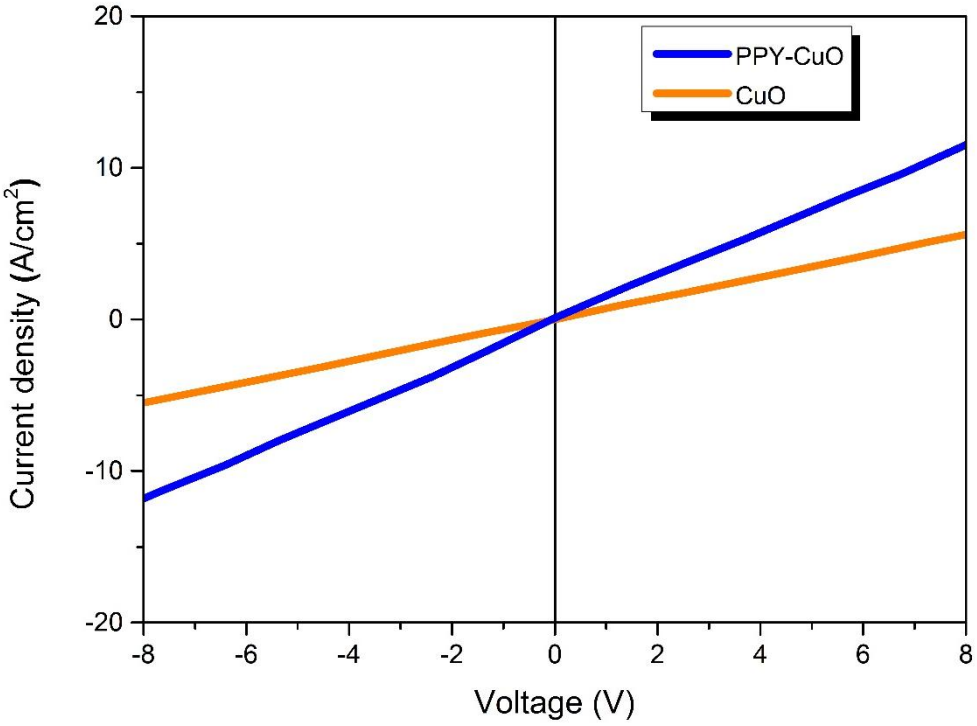

Fig. 5: Current density-voltage (J-V) spectrafor CuO,and PPY-CuOnanocomposite.

4. Conclusions

The nanocomposite materials CuO, PPY and PPY-CuO, were created by chemical oxidative polymerization. The shift in bond length that happened simultaneously with the change in nano-strain served as evidence that the CuO, PPY and PPY-CuOnanocomposite were effectively synthesized.The FESEM and TEM pictures of PPY-CuO nanocomposites

revealed extensive loading of PPY matrices with non-homogeneous distribution of CuO. The average particle size for PPY-CuO nanocomposites in TEM images was determined to be 46 nm, which was found to be in good agreement with FESEM images. The XRD spectra, which featured an amorphous band of PPY, and crystalline peaks of CuO nanoparticles, supported the synthesis of PPY-CuO nanocomposites. It was widely acknowledged that the XRD findings confirmed the FESEM results. The maximum rate of radiative charge (electron-hole) carrier recombination was observedfor PPY-CuO nanocomposites as inferred by PL spectra. When compared to pure CuO, the J-V characteristics of the PPY-CuO nanocomposite showed an improvement in the current density, with an optimized higher current density of 11.36 A/cm^2. Due of its high electrical conductivity, increased non-radiative recombination rate, improved electron mobility and increased luminescence in the visible spectrum, the PPY-CuO nanocomposite was proposed to be an intriguing electron transport layer material for OLED devices.

Acknowledgements

Authors express their sincere thanks to IIIT Ranchi and IIT-ISM Dhanbad for their administrative support. This research did not receive any specific grant from funding agencies in the public, commercial, or not-for-profit sectors. Authors also acknowledge DST, New Delhi for using lifetime spectrometer (project no. SR/FST/PSI-004/2013).

References

[1] X. Li, F. Xie, S. Zhang, J. Hou, W. CH Choy, MoOx and V2Ox as hole and electron transport layers through functionalized intercalation in normal and inverted organic optoelectronic devices, Light: Science & Applications, 4 (2015) e273– 1-7.

[2]M.C. Gather, A. Kohnen, K. Meerholz, White Organic Light-Emitting Diodes, Adv. Mater., 23 (2011) 233–248.

[3] L. Xiao, Z. Chen, B. Qu, J. Luo, S. Kong, Q. Gong, J. Kido, Recent progresses on materials for electrophosphorescent organic light-emitting devices, Adv. Mater., 23 (2011) 926-952.

[4] G. P. Crawford, Flexible Flat Panel Displays, 2005, DOI: 10.1002/0470870508.ch1, pp. 1-9. 2.

[5] R.H. Friend, R.W. Gymer, A.B. Holmes, J.H. Burroughes, R.N. Marks, C. Taliani, D.D.C. Bradley, D.A. Dos Santos, J.L. Bredas, M. Logdlund, W. R. Salaneck, Electroluminescence in conjugated polymers, Nature, 397 (1999) 121-128.

[6] J. Zou, H. Wu, C.-S. Lam, C. Wang, J. Zhu, C. Zhong, S. Hu, C.-L. Ho, G.-J. Zhou, H. Wu, W.C.H. Choy, J. Peng, Y. Cao, W.-Y. Wong, Simultaneous optimization of charge-carrier balance and luminous efficacy in highly efficient white polymer light-emitting devices, Adv. Mater. **23** (2011) 2976–2980.

[7] H. Sasabe, J. Kido, Development of high-performance OLEDs for general lighting, J. Mater. Chem. C 1 (2013) 1699-1707.

[8] M. L. Hildner, in Flexible Flat Panel Displays, 2005, DOI: 10.1002/0470870508.ch15, pp. 285-312.

[9] H.W. Choi, S.Y. Kim, W.-K. Kim, J.-L.Leea, Enhancement of electron injection in inverted top-emitting organic light-emitting diodes using an insulating magnesium oxide buffer layer, Appl. Phys. Lett. 86 (2005) 012104.

[10] C.-I. Wu, C.-T. Lin, Y.-H. Chen, M.-H. Chen,Electronic structures and electron-injection mechanisms of cesium-carbonate-incorporated cathode structures for organic light-emitting devices, Appl. Phys. Lett. 88 (2006) 152104.

[11] J. Liu, G.Z. Cao, Z.G. Yang, D.H. Wang, D. Dubois, X.D. Zhou, G.L. Graff, L.R. Pederson, J.G. Zhang, Oriented Nanostructures for Energy Conversion and Storage, ChemSusChem.1 (2008) 676- 697.

[12] K. Sharma, V. Sharma, S. S. Sharma, Dye-Sensitized Solar Cells: Fundamentals and Current Status, Nanoscale Res. Lett. 13 (2018) 381.

[13] K.Y. Xie, J. Li, Y.Q. Lai, W. Lu, Z. Zhang, Y.X. Liu, L. Zhou, H.T. Huang, Highly ordered iron oxide nanotube arrays as electrodes for electrochemical energy storage, Electrochem. Commun. 13 (2011) 657-660.

[14]P.J. Hall, M. Mirzaeian, S.I. Fletcher, F.B. Sillars, A.J. Rennie, G.O. ShittaBey, G.Wilso n, A. Cruden, R. Carter, Energy storage in electrochemical capacitors: designing functional materials to improve performance, Energy Environ. Sci. 3 (2010) 1238-1251.

[15] J. Dong, Y. Lin, H. Zong, H. Yang, Hierarchical $LiFe_5O_8$@PPy core-shell nanocomposites as electrode materials for supercapacitors, Appl. Surf. Sci. 470 (2019) 1043-1052.

[16] C.-S. Ha, Polymer Based Hybrid Nanocomposites; A Progress Toward Enhancing Interfacial Interaction and Tailoring Advanced Applications, Chem. Rec. 18 (2017), 759-775.

[17] V. Resta, L. Calcagnile, G. Quarta, L. Maruccio, A. Cola, I. Farella, G. Giancane, L. Valli, Optical and electrical properties of polycarbonate matrices implanted by high energy Cu ions, Nucl. Instr. Meth. Phys. Res. B 312 (2013) 42–47.

[18] J. Stejskal, R.G. Gilbert, Polyaniline. Preparation of a conducting polymer, Pure Appl. Chem. 74 (2002) 857-867.

[19] V. Saxena, D.K. Aswal, M. Kaur, S.P. Koiry, S.K. Gupta, J.V. Yakhmi, R.J. Kshirsagar, S.K. Deshpande, Appl. Phys. Lett. 90 (2007) 043516.

[20] B. Balamurugan, B.R. Mehta, Optical and structural properties of nanocrystalline copper oxide thin films prepared by activated reactive evaporation, Thin Solid Films 396 (2001)90–96.

[21]. J. Ghijsen, L.H. Tjeng, J.V. Elp, H. Eskes, J. Westerink, G.A. Sawatzky, Electronic structure of Cu_2O and CuO, Phys Rev B 38 (1988)11322-11330.

[22] R Kandulna, RB Choudhary, P Maji, Ag-doped ZnO reinforced polymeric Ag: ZnO/PMMA nanocomposites as electron transporting layer for OLED application, J. Inorg. Organomet. Polym.27 (2017) 1760-1769.

[23] R. Kandulna, R.B. Choudhary, Robust electron transport properties of PANI/PPY/ZnO polymeric nanocomposites for OLED applications, Optik, 144 (2017), 40-48.

[24] Y.-W. Hsu, T.-K. Hsu, C.-L. Sun, Y.-T. Nien, N.-W. Pu, M.-D. Ger, Synthesis of CuO/graphene nanocomposites for nonenzymatic electrochemical glucose biosensor applications. Electrochim. Acta, 82 (2012) 152–157.

[25] R. Kandulna, R.B. Choudhary, 2-D rGO impregnated circular-tetragonal-bipyramidal structure of PPY-TiO2-rGO nanocomposite as ETL for OLED and supercapacitor electrode materials, Mater. Sci. Semiconducting Process. 94 (2019) 86-96

[26] S. Gnanam, V. Rajendran,Synthesis of CeO_2 or α–Mn_2O_3 nanoparticles via sol–gel process and their optical properties, J. Sol-Gel. Sci. Technol. 58 (2011), 62-69.

[27] B.P. Zhang, N.T. Binh, K. Wakatsuki, Y. Segawa, Y. Kashiwaba, and K. Haga, Synthesis and optical properties of single crystal ZnO nanorods, Nanotechnology, 15(2004)S382–S388.

[28]M.A. Subhan, N.Uddin, P. Sarker, A.K. Azad, K. Begum, Photoluminescence, photocatalytic and antibacterial activities of CeO_2·CuO·ZnO nanocomposite fabricated by co precipitation method, Spectrochim. Acta A Mol. Biomol. Spectrosc. 149 (2015) 839-850.